Anisotropic and Nonhomogeneous Thermal Conduction in 1 μm Thick CVD Diamond

Aditya Sood[1,2], Jungwan Cho[1], Karl D. Hobart[3], Tatyana Feygelson[3], Bradford Pate[3], Mehdi Asheghi[1], Kenneth E. Goodson[1]

[1]Department of Mechanical Engineering,
[2]Department of Materials Science and Engineering,
Stanford University
Stanford, CA, USA, 94305
Email: aditsood@stanford.edu

[3]Naval Research Laboratory
Washington, DC, USA, 20375

ABSTRACT

We present an experimental study of thermal conduction in 1 μm thick suspended CVD diamond film by time-domain thermoreflectance (TDTR), an optical pump-probe technique. Important aspects of signal analysis and measurement sensitivity are discussed, outlining the various thermal metrology challenges posed by this system. We measure the properties of the near-interfacial coalescence region and high-quality growth region by performing experiments on the bottom and top sides of the suspended film, respectively, and find that the small average grain size of the former, and strong columnar anisotropy of the latter region are reflected in the measurements of thermal conductivity. Our TDTR methodology utilizes the information present in both the amplitude and phase response of the system at the modulation harmonic of the pump laser, in order to separate out the effects of the transducer-diamond thermal boundary conductance from the intrinsic diamond conductivity. Additionally, measurements are made across a range of modulation frequencies in order to obtain better estimates of the conductivity anisotropy. For the 1 μm thick film, we estimate an in-plane to through-plane anisotropy ratio of ~ 0.3, and through-plane conductivities of ~ 440 W/m-K and ~ 140 W/m-K for the high quality and coalescence regions, respectively.

KEY WORDS: CVD diamond, heat spreaders, coalescence and growth, columnar anisotropy, thermal boundary resistance (TBR), time-domain thermoreflectance (TDTR)

NOMENCLATURE

C	volumetric specific heat ($Jm^{-3}K^{-1}$)
L	thermal penetration depth (m)
V	voltage signal (V)
f	frequency (Hz)
k	thermal conductivity ($Wm^{-1}K^{-1}$)

Greek symbols

α	thermal diffusivity (m^2s^{-1})
η	conductivity anisotropy

Subscripts

HQ	high-quality
IF	interfacial
r	radial (lateral/ in-plane)
z	vertical (through-plane)
v	volumetric (specific heat)
in	in-phase
out	out-of-phase
mod	modulation
p	penetration (depth)

INTRODUCTION

Diamond has emerged as a promising heat sink material in several niche applications involving high heat-flux hot spots. This is due to its extremely high thermal conductivity in bulk, single-crystalline form, which may be as much as 3000 W/m-K at room temperature. However, commercial diamond substrates are commonly grown synthetically using processes such as chemical vapor deposition (CVD). CVD is based on a nucleation and growth process, and results in diamond films with a polycrystalline grain structure. Nucleation and coalescence create near-interface regions of small grain size, and consequently low thermal conductivity, while grain growth results in higher quality regions away from the interface with higher conductivity [1][2]. Moreover, the columnar texture of the latter region results in a highly anisotropic conductivity tensor, with a lower conductivity in-plane as compared to through-plane [3]. The measurement of the conductivity and anisotropy of these different regions within a film is important for two main reasons. First, it provides accurate data to model thermal effects in devices, enabling more reliable predictions of their performance, reliability and life-time. Second, it helps in the optimization of CVD growth parameters that result in the highest quality material with smallest thermal resistances. Previous efforts to measure the nonhomogeneous and anisotropic thermal properties of CVD diamond have focused on the characterization of samples with large film thicknesses (exceeding 10 μm) [4], [5], and reported anisotropy ratios (in-plane to through-plane conductivity) in the range 0.5-0.8. In this work, we measure the nonhomogeneous and anisotropic thermal conduction in a suspended 1 μm CVD diamond film using time-domain thermoreflectance (TDTR), an optical pump-probe technique. We first discuss the various challenges associated with the metrology of such films with complex microstructure, from the point of view of signal interpretation and measurement sensitivity. We then present TDTR data, and interpretation guided by our sensitivity analysis. We find that the data are consistent with an in-plane to through-plane anisotropy ratio close to 0.3, and through-plane conductivities of around 440 W/m-K and 140 W/m-K for the high-quality

columnar and near-interfacial coalescence regions, respectively.

TDTR SETUP

TDTR is a well-established optical technique used to measure the thermal properties of thin films. Our setup is built around a 1064 nm Nd-YVO_4 mode-locked laser (Time-Bandwidth products) that emits ~ 9 ps wide pulses at a repetition rate of 82 MHz. Pump pulses are amplitude modulated at a frequency f_{mod} (typically between 1-10 MHz) using an electro-optic modulator (Conoptics M360-80), and frequency doubled to 532 nm using a periodically poled $LiNbO_3$ crystal. While the pump pulses travel a fixed path, the probe pulses travel a path of variable path length that includes an optical delay stage. The pump pulses are used to heat up the sample via photo-thermal energy conversion in a thin Al coating (~50 nm), while the time-delayed (0 to 3.5 ns) probe pulses are used to interrogate the transient changes in the reflectivity of the Al film. The output signals from the experiment are the in- and out-of-phase voltage components of the reflected probe intensity at the first harmonic of the modulation frequency, V_{in} and V_{out} measured using an SRS 844 lock-in amplifier (Stanford Research Systems). The unknown thermal properties can be extracted by fitting the *amplitude*, $R = (V_{in}^2 + V_{out}^2)^{0.5}$ or the *ratio* (tangent of phase angle) $r = -V_{in}/V_{out}$ data to a multilayer thermal diffusion model that accounts for radial heat spreading, anisotropic thermal conductivities, and finite thermal interface conductance [6]. Pump and probe laser spot sizes of 10 µm and 6 µm, respectively, were used in these experiments.

SAMPLE DESIGN

The sample consists of a 1 µm thick diamond film grown by microwave plasma CVD on a silicon substrate. Prior to growth, the substrate was seeded in an ethanol based suspension prepared using detonation nanodiamond powder. The nanodiamond material is characterized by a high degree of grain size homogeneity, with an average particle size of 4.0 nm. The seeding was carried out through an ultrasonic treatment in the nanodiamond suspension followed by an ethanol rinse and immediate spin-dry, resulting in a uniform initial seed density of $> 10^{12}$ nuclei/cm^2 [7]. CVD growth was carried out in an ASTEX 1.5 kW microwave plasma deposition system using purified methane and hydrogen as reactant gases, with the methane to hydrogen ratio varied from 0.7% during film coalescence to 0.3% during the remaining diamond deposition. The growth parameters were: 15 torr, 750º C, 800 Watts. The initial stage of deposition consists of film growth from the dispersed nanodiamond seeds, without re-nucleation. The resulting diamond film comprises crystallites with a columnar structure normal to the growth interface; survival of the competing grains causes the lateral grain size to increase with the film thickness. The coalescence region is estimated to be ~300 nm, which is the thickness at which the films are pinhole free. The presence of pinholes is checked by treating diamond films grown on oxidized silicon wafers with buffered HF, and observing etch-pits in the underlying oxide through optical microscopy.

. The central (~5 mm diameter) portion of the film was suspended by back-etching the silicon in order to provide direct experimental access to the coalescence region. The sample was coated from the top and bottom sides with a 50 nm thick aluminum film that acts as a transducer for TDTR measurements (see Figure 1).

METROLOGY – THEORETICAL ANALYSIS OF SENSITIVITY

As discussed above, the complex microstructure of CVD diamond results in a nonhomogeneous and anisotropic variation of the thermal conductivity within the thickness of the film. Any thermal measurement technique averages over the properties of material within a finite volume depending on the characteristic length scale of its probe. This poses a challenge to the correct interpretation of conductivity data. In this section, we perform theoretical sensitivity analyses to show how various sample properties of interest affect TDTR data, and what strategies may be adopted to extract meaningful information from them.

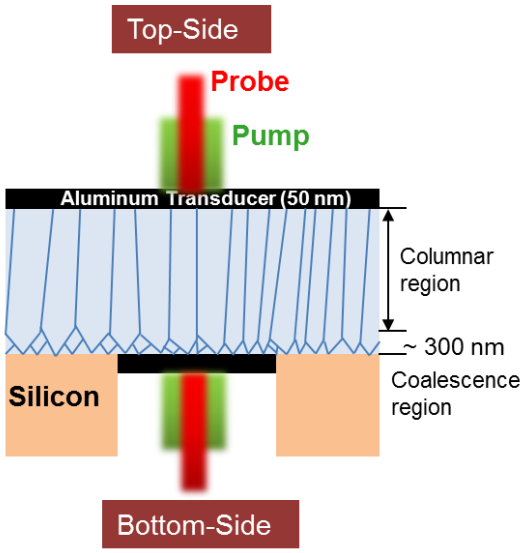

Fig 1 Sample schematic in cross-section

Amplitude versus Phase (or Ratio) Data

The amplitude (R) and ratio (r) of the voltage signal generated by the reflected probe light at the modulation harmonic are sensitive in different measures to different thermal properties within a sample stack. These properties include the thickness, through- and in-plane thermal conductivity and specific heat of constituent layers, and the thermal boundary resistance (TBR) of interfaces between layers. To enable a quantitative analysis, we define the sensitivity coefficients S_β as follows

$$S_\beta = \frac{\partial \log(\gamma)}{\partial \log(\beta)} \quad , \qquad (1)$$

where γ is either the amplitude R or ratio r, and β is one of the thermal properties listed above. The value of the sensitivity coefficient is a function both of the modulation frequency and

the probe delay time. A large magnitude of S_β indicates that the measurement is sensitive to the property β, while a value close to zero means that it is insensitive. In the following section, we theoretically analyze the sensitivity of TDTR measurements in different scenarios, starting from a typical homogeneous isotropic film on substrate, including the effects of non-homogeneity, finally leading up to the case of a suspended anisotropic film.

Case a) Homogeneous and isotropic film on substrate. This case corresponds to the most common application, wherein a film may be epitaxially grown or deposited on top of a substrate. The film is thermally isotropic and homogeneous. The sample configuration modeled here consists of a 1 µm film (k_{Film} = 10, 100, 1000 W/m-K; C_v = 1.8 MJ/m^{3}K) on a semi-infinite silicon substrate (k = 140 W/m-K, C_v = 1.86 MJ/m^{3}K), coated with a 50 nm aluminum transducer film. The baseline values for the TBR at the interfaces between the aluminum/film and film/substrate are taken to be 15 m^{2}K/GW. The modulation frequency of the pump is taken to be 6 MHz.

In Figure 2 we plot the sensitivity coefficients for the conductivity of the film k_{Film} and the TBR at the Al/film interface as a function of probe delay time. Since these two quantities are fitted simultaneously, the accuracy with which the two can be extracted independently depends on their relative sensitivity coefficients.

The plots show that at low to intermediate values of k_{Film}, both the amplitude and ratio provide sufficient sensitivity to simultaneously extract the Al/film TBR and k_{Film}. However, when the conductivity of the film exceeds about 100 W/m-K, the amplitude signal becomes increasingly sensitive to the TBR and insensitive to k_{Film} such that the two quantities cannot be accurately separated by a single measurement. The ratio signal on the other hand provides sufficient sensitivity to k_{Film} even for highly conducting films.

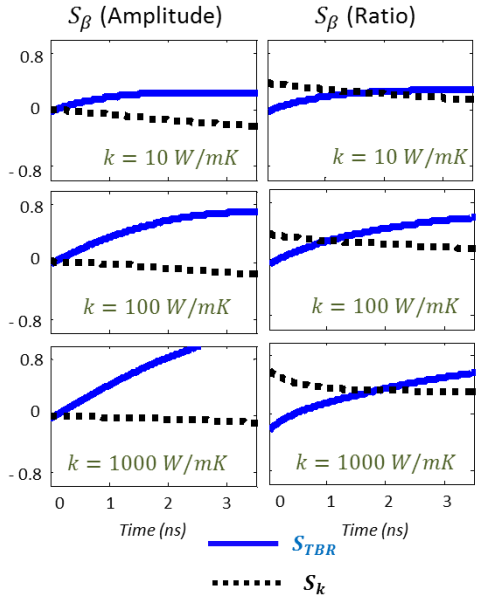

Fig 2 Sensitivity analysis for an isotropic film on substrate corresponding to Case (a)

Case b) Two-layer nonhomogeneous film on substrate. We now consider the case where the film consists of sub-layers with different thermal conductivities. The sub-layers themselves are locally isotropic. This case models the morphology that might result from the nucleation and growth of a polycrystalline material comprising equiaxed grains, or from the growth of a film with a disordered near interfacial region. Here, the film is modeled as comprising two sub-layers, a 200 nm thick low conductivity near-interfacial layer (k_{IF} = 10 W/m-K) and an 800 nm thick high-quality layer (k_{HQ} = 40 W/m-K). All other material parameters are identical to those in Case (a).

We examine the sensitivity of the amplitude and ratio signals to k_{IF} and k_{HQ}. The analysis is performed at two different modulation frequencies: 1 MHz and 10 MHz. The modulation frequency of the pump laser f_{mod} determines the thermal penetration depth: $L_p \sim \sqrt{\alpha / \pi f_{\mathrm{mod}}}$ where α is the thermal diffusivity of the sample given by k/C_v. Smaller modulation frequencies enhance the measurement sensitivity to thermal properties of buried films and interfaces, while higher modulation frequencies enhance the sensitivity to properties of films and interfaces that are closer to the heat source.

As shown in Figure 3, the ratio signal is more sensitive to the properties of the buried near-interfacial region (k_{IF}) as compared to the amplitude, which is almost insensitive to it even at the lower modulation frequency. We also see that the sensitivity to k_{IF} is higher at the lower modulation frequency both in the amplitude and ratio signals, consistent with the fact that the penetration depth scales inversely with f_{mod}.

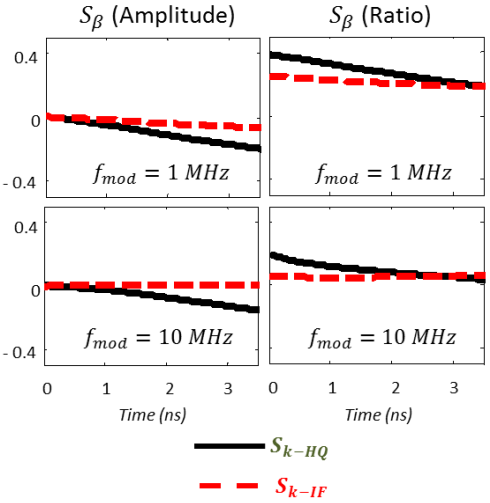

Fig 3 Sensitivity analysis for a two-layer nonhomogeneous film on substrate, corresponding to Case (b)

Case c) Anisotropic film on substrate. We now examine the case of a film whose thermal conductivity tensor is anisotropic, i.e. whose conductivity in the through-plane direction is different from that in the in-plane direction. Such a scenario might arise for instance in the case of a polycrystalline film, whose grains are oriented in a columnar fashion with the long axis pointing in the film-normal direction, or even simply in a crystalline film with an inherently non-cubic lattice structure. We analyze the

sensitivity of the amplitude and ratio signals to the in- and through-plane conductivities k_r and k_z of the film. The model considered here is identical to that in Case (a) in all respects apart from the anisotropic nature of the film's conductivity; k_r and k_z are taken to be 60 W/m-K and 100 W/m-K respectively. No division into near-interfacial and high-quality regions is taken into account, i.e. the film is assumed to be homogeneous.

The sensitivity plots in Figure 4 show that while both the amplitude and ratio signals are reasonably sensitive to k_z, they differ in their relative sensitivities to the in-plane conductivity k_r. While the amplitude is almost insensitive to k_r at both low and high modulation frequencies, the ratio is sensitive to k_r at low frequencies. Lower f_{mod} correspond to greater in-plane thermal spreading, thereby making the temperature oscillations dependent on the lateral thermal conductivity.

Case d) Anisotropic film – suspended. Here we consider the case that corresponds closely with our experiment, in which the silicon substrate in Case (c) has been back-etched resulting in a suspended film. The conductivity tensor in the film is identical to that in (c) with k_r = 60 W/m-K and k_z = 100 W/m-K, i.e. an anisotropy ratio of 0.6. The film is coated on the top-side with a 50 nm thick Al layer, and suspended in air (k = 0.03 W/m-K, C_v = 1000 J/m^{3}K). In Figure 5 we analyze the sensitivity of the ratio and amplitude signals to k_r and k_z.

The qualitative comparison between the amplitude and ratio signals is similar to Case (c). At low f_{mod} the ratio signal is sensitive to the in-plane conductivity k_r while at high f_{mod}, both the amplitude and ratio are sensitive only to k_z. However, we note the difference in magnitudes of sensitivity coefficients between Figures 4 and 5. A measurement of the suspended film yields a larger sensitivity to the in-plane conductivity than in the on-substrate film. Qualitatively, this is due to the fact that heat is confined to a far greater extent within the film and forced to spread laterally when it is in contact with air (k = 0.03 W/m-K) as compared to when it is on silicon (k = 140 W/m-K).

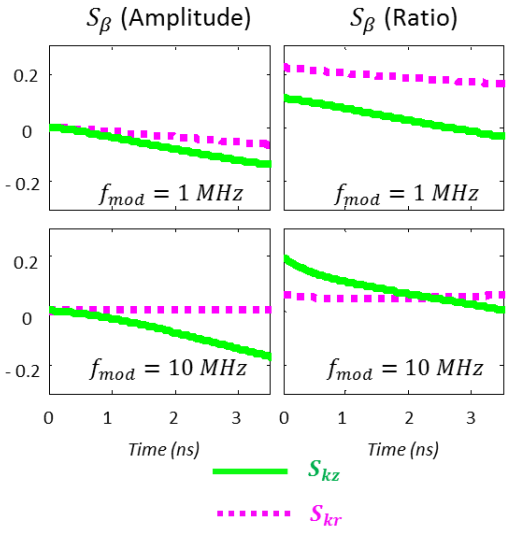

Fig 4 Sensitivity analysis for an anisotropic film on substrate, corresponding to Case (c)

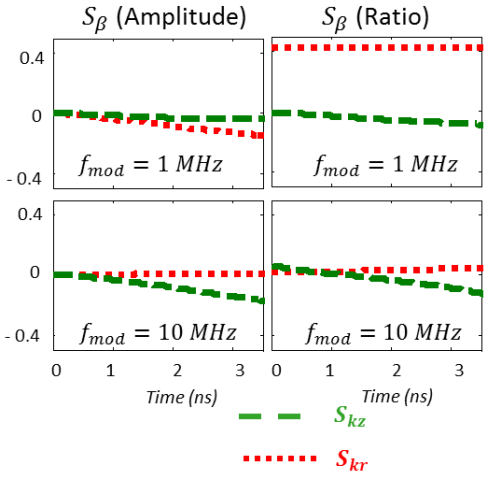

Fig 5 Sensitivity analysis for a suspended anisotropic film, corresponding to Case (d)

The main findings of this section are summarized below:

1. For homogeneous and isotropic films with low to intermediate conductivity, both the amplitude and ratio signals provide sufficient sensitivity to extract the film conductivity and Al-film TBR in a simultaneous fit. However, for films with high conductivity, the amplitude signal is dominated by the TBR.
2. For films that are non-homogeneous with depth, the ratio signal is more sensitive to properties of buried sub-layers. This is more pronounced at lower modulation frequencies, as the corresponding thermal penetration depth is larger.
3. The ratio is more sensitive to the in-plane conductivity of a film as compared to the amplitude. The effective (isotropic) conductivity of a film with a columnar grain structure (with $k_r < k_z$) extracted using the ratio signal would therefore be smaller than that measured using the amplitude signal. The former would be a direction averaged value lying between k_r and k_z, while the latter would be closer to k_z. This is more so at lower modulation frequencies, where the lateral spreading of heat is greater.
4. Suspended films provide far greater sensitivity to in-plane properties as compared to on substrate. This is a direct consequence of the confinement of heat within the film and enhanced conduction in the lateral direction.

We now employ our understanding of TDTR signal types and their sensitivity to various sample properties to the measurement of thermal conductivity in thin film CVD diamond.

EXPERIMENTAL RESULTS AND DISCUSSION

Bottom-Side (Nucleation Region) Measurements

TDTR measurements were performed on the bottom-side of the diamond film, for direct access to the thermal properties of the coalescence region. Thermal decay traces were taken at four different modulation frequencies: 2, 4, 6 and 8 MHz. The TBR at the interface between the Al transducer and bottom-

side of the diamond film ("bottom-side TBR") was found by fitting the amplitude data, owing to its larger sensitivity to this quantity compared to the ratio data. Its value was found to be ~21.2 m^2K/GW, fairly independent of f_{mod}, suggesting that it was extracted independently of the conductivity. Using this value of TBR, the ratio data was fit for the thermal conductivity of diamond. It was seen that the data did not fit well when the diamond film was assumed to be isotropic. Good fits were obtained by allowing both the through-plane conductivity k_z and the anisotropy ratio η $(=k_r/k_z)$ to vary as free parameters (see Fig 6). The best fit values for k_z and η are plotted in Figure 7a,b as a function of f_{mod}. Averaged over all frequencies we get values of k_z = (139 ± 12) W/m-K and η = (0.31 ± 0.13).

Top-Side (High-Quality Region) Measurements

Similar measurements were performed on the top-side, for thermal access to the properties of the high-quality columnar region. The TBR at the top interface between the Al transducer and high-quality diamond ("top-side TBR") was found to be ~8.4 m^2K/GW using the same methodology as above. The difference between the top-side and bottom-side Al/Diamond TBRs is not entirely unexpected. While this difference may be due to variations in sample surface conditions alone, the higher resistance of the bottom interface may also be a result of the low thermal conductivity of the near-interfacial region, consisting of the nucleation layer and small grained coalescence region.

Using the value of the top TBR = 8.4 m^2K/GW, the ratio data were used to extract diamond conductivity. Similar to the measurements made on the bottom-side, it was found that the data fit poorly when the film was assumed to be isotropic. Fitting both k_z and η as free parameters led to good fits (see Fig 6), at all f_{mod}. Best fit pairs of k_z and η are plotted in Figure 7a,b. Averaged over all frequencies, the through-plane conductivity and anisotropy ratio are k_z = (440 ± 55) W/m-K and η = (0.30 ± 0.11).

Therefore, we find that values of η in the range 0.2 to 0.4 consistently fit data taken from the top and bottom sides of the film. This strong anisotropy in conductivity is a result of a highly columnar grain structure with the long axes of the grains oriented in the film-normal direction. Fewer grain boundaries impede the transport of phonons in the vertical direction as compared to in-plane, leading to a larger conductivity in the former. Further, we note that the through-plane conductivity measured on the top-side is ~3 times that measured on the bottom-side. This is consistent with the highly non-homogeneous microstructure present within the first few µm of CVD diamond. The high concentration of grain boundaries and smaller average grain size in the coalescence region lead to large amounts of phonon scattering, and low thermal conductivity. Average grain size (both in the vertical and horizontal directions) increases with distance from the growth substrate, and hence so does the local conductivity. The measurement averages the thermal properties of the film over the characteristic thermal penetration depth L_p. Using the through-plane conductivities measured from the top and bottom-side, L_p is found to be between 1.8 µm (at 8 MHz) and 3.5 µm (at 2 MHz) for measurements made from the bottom-side and between 3 µm (at 8 MHz) and 6 µm (at 2 MHz) for measurements made from the top-side. We note that the actual thermal penetration depth is likely smaller than this, as the expression $L_p \sim \sqrt{\alpha / \pi f_{\mathrm{mod}}}$ provides good estimates of diffusion depth in semi-infinite media. At best, L_p gives an order of magnitude length scale for thermal penetration into the diamond film in our case. Given that L_p is comparable to the film thickness (1 µm), the extracted values of conductivity are averaged over the entire film thickness. However, this is a weighted average with greater weight given to material closer to the laser spot, explaining why a smaller effective conductivity is measured from the bottom side. A larger fraction of high-quality columnar diamond would lead to a larger difference between the through-plane conductivity values measured from the top and bottom sides.

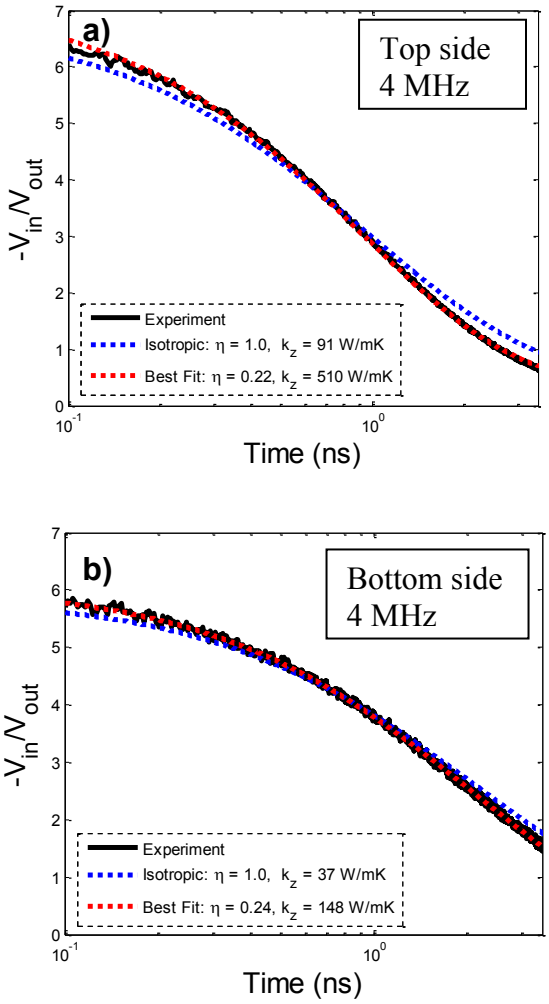

Fig 6 TDTR ratio data and fits to the isotropic and anisotropic models for measurements taken from the (a) top-side and (b) bottom-side, at f_{mod} = 4 MHz. In either case, the best fit is obtained by allowing both the through-plane conductivity and anisotropy ratio to vary as free parameters. A lower conductivity in-plane compared to through-plane (η < 1) is required to correctly explain the data, consistent with the columnar anisotropy of CVD diamond films.

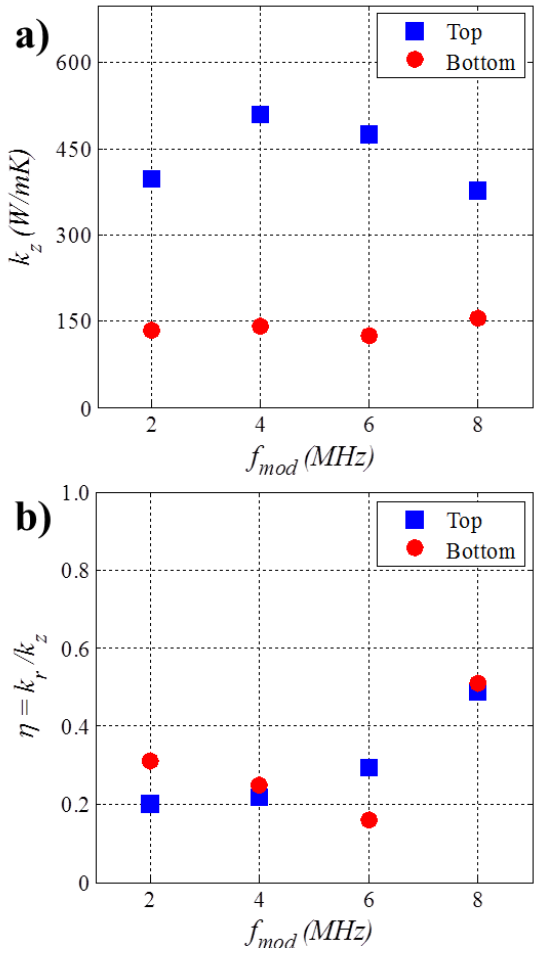

Fig 7 a) Through-plane thermal conductivity and b) Anisotropy ratio of 1 µm thick suspended CVD diamond film, measured from the top and bottom sides.

In a recent paper [2] similar measurements were reported by us on the same set of samples, where the thermal conductivity of the 1µm thick sample was found to be 80 W/m-K as measured from the bottom-side. This measurement was made using the amplitude data, at a modulation frequency of 5 MHz. The difference between this earlier data point and the values reported here is due to the fact that we assumed the diamond film was isotropic; therefore, 80 W/m-K is a direction averaged value lying between the in-plane (~40 W/m-K) and through-plane (~140 W/m-K) conductivities extracted here.

CONCLUSIONS

The thermal metrology of diamond films presents a unique challenge, due to the complex nature of the material's microstructure and the manner in which the transport of phonons is affected by the local density of defects. Optical techniques such as TDTR provide a useful platform to probe the thermal properties of these materials at small length scales, in a non-destructive manner. Studies in the past typically used two or more techniques in tandem to measure the anisotropy of diamond films, such as the transient thermal grating (TTG) method to measure in-plane and the laser-flash technique to measure through-plane conductivity [8][9]. Here, through careful experimental design and signal interpretation, we have used a single technique to obtain an estimate of these properties. We obtained approximate values of the anisotropy ratio of between 0.2-0.4 for a 1 µm thick film, and showed how the non-homogeneity in grain size is reflected in measurements of thermal conductivity. Ongoing and future work includes improving the methodology to enhance measurement accuracy, and correlating the thermal data with material properties obtained through microstructural and other characterization means.

ACKNOWLEDGEMENTS

The authors gratefully acknowledge financial support from the Air Force Office of Scientific Research (agreement # FA9550-12-1-0195, titled: Multi-Carrier and Low-Dimensional Thermal Conduction at Interfaces for High Power Electronic Devices) and the Defense Advanced Research Projects Agency's Microsystems Technology Office through the Near Junction Thermal Transport program. Research performed at the Naval Research Laboratory is supported by the Office of Naval Research. The authors acknowledge fruitful discussions on an earlier data set with collaborators at Northrop Grumman Corporation.

References

[1] K. E. Goodson, "Thermal conduction in nonhomogeneous CVD diamond layers in electronic microstructures," *J. Heat Transfer*, vol. 118, no. May, 1996.

[2] E. Bozorg-Grayeli, A. Sood, M. Asheghi, V. Gambin, R. Sandhu, T. I. Feygelson, B. B. Pate, K. Hobart, and K. E. Goodson, "Thermal conduction inhomogeneity of nanocrystalline diamond films by dual-side thermoreflectance," *Appl. Phys. Lett.*, vol. 102, no. 11, 2013.

[3] J. E. Graebner, S. Jin, G. W. Kammlott, B. Bacon, L. Seibles, and W. Banholzer, "Anisotropic thermal conductivity in chemical vapor deposition diamond," *J. Appl. Phys.*, vol. 71, no. 11, pp. 5353–5356, 1992.

[4] J. E. Graebner, S. Jin, G. W. Kammlott, J. A. Herb, and C. F. Gardinier, "Large anisotropic thermal conductivity in synthetic diamond films," *Nature*, vol. 359, pp. 401–403, 1992.

[5] J. E. Graebner, M. E. Reiss, L. Seibles, T. M. Hartnett, R. P. Miller, and C. J. Robinson, "Phonon scattering in chemical-vapor-deposited diamond," *Phys. Rev. B*, vol. 50, no. 6, 1994.

[6] D. G. Cahill, “Analysis of heat flow in layered structures for time-domain thermoreflectance,” *Rev. Sci. Instrum.*, vol. 75, no. 12, p. 5119, 2004.

[7] J. Philip, P. Hess, T. Feygelson, J. E. Butler, S. Chattopadhyay, K. H. Chen, and L. C. Chen, “Elastic, mechanical, and thermal properties of nanocrystalline diamond films,” *J. Appl. Phys.*, vol. 93, no. 4, p. 2164, 2003.

[8] E. V Ivakin, A. V Sukhodolov, V. G. Ralchenko, A. V Vlasov, and A. V Khomich, “Measurement of thermal conductivity of polycrystalline CVD diamond by laser-induced transient grating technique,” *Quantum Electron.*, vol. 32, no. 4, pp. 367–372, Apr. 2002.

[9] A. V Sukhadolau, E. V Ivakin, V. G. Ralchenko, and A. V Khomich, “Thermal conductivity of CVD diamond at elevated temperatures,” *Diam. Relat. Mater.*, vol. 14, pp. 589–593, 2005.